Journal of Engineering and Technology for Industrial Applications

ITEGAM-JETIA

Manaus, v10. n.50, p. 103-111. November/ December., 2024.
DOI: https://doi.org/10.5935/jetia.v10i50.1354

ISSN ONLINE: 2447-0228

RESEARCH ARTICLE OPEN ACCESS

# MACHINING PARAMETERS OPTIMIZATION IN WET TURNING OF EN31 MATERIAL USING BOX-BEHNKEN APPROACH OF RSM

**Shivaji Bhivsane[1], Arvind Chel[2], Siraj Sayyed[3]**

[1] Research Scholar, Dr. Babasaheb Ambedkar Marathwada University, Aurangabad-431004, (MH) India.
[2] Department of Mechanical Engineering, Jawaharlal Nehru Engineering College, Aurangabad-431001, (MH) India.
[3] Department of Mechanical Engineering, Maharashtra Institute of Technology, Aurangabad-431010, (MH) India.

[1] https://orcid.org/0000-0002-1169-957X, [2] https://orcid.org/0000-0001-7817-8958, [3] https://orcid.org/0000-0001-8531-7258

Email: bhivsanesv@gmail.com, achel@mgmu.ac.in, lucky.sartaj@gmail.com

**ARTICLE INFO**

***Article History***
Received: October 26, 2024
Revised: November 6, 2024
Accepted: November 10, 2024
Published: November 30, 2024

***Keywords:***
EN31 Material,
Wet Turning,
RSM,
Tribological Parameters,
Surface Finish,
Optimization.

**ABSTRACT**

Manufacturing sectors are always challenged to enhance surface quality and tool life while reducing machining costs and setup times in hard-turning operations. In line with this, the current study focused on surface roughness optimization employing machining parameters such as cutting speed: ν (160-260 m/min), feed: f (0.1-0.2 mm/rev), depth of cut: d (0.05-0.15 mm), and tool nose radius: re (0.4-1.2 mm) as functions. The experiment was designed by using Box-Behnken approach of RSM and carried out on a commercial CNC machine using EN31 material at 47 HRC. The research found that machining parameters have a considerable effect on surface roughness, as do stresses, vibrations, heat generation, and increased material per pass. The experimental surface roughness observed in between 1.34-2.81 µm whereas estimated surface roughness have R2=0.9976. The Anova design model showed face value of 356.21 which indicates the developed model is noteworthy. The significant and marginal effect of machining parameters are evaluated by considering p-value and overcall error observed within the range of 1.613-1.974%..



## I. INTRODUCTION

In recent years, turning operations have garnered a lot of attention in the machining of hard materials with hardnesses more than 45 HRC [1]. Hard machining involves material hardness ranging from 45 to 68 HRC, and the steel is classed as alloy, tools, hardened, hard-chrome, and heat-treated steels [2]. To turn such workpiece materials, turning inserts such as carbide, ceramics, CBN, and PCBN must have extremely high mechanical and thermal load capacities [3]. Hard turning has many advantages over grinding, including lower costs, faster and easier execution, and nearly identical surface roughness [4],[5]. Several elements influence the behavior of the cutting process, including tool variables, workpiece variables, and cutting circumstances such as material, mechanical properties, chemicals, and physical characteristics [6]. The selection of ideal process parameters is typically a challenging task, but it is a critical aspect of machining process management in order to achieve enhanced product quality, high productivity, and low cost. The optimization of machining parameters using experimental approaches and mathematical and statistical models has expanded significantly over time to meet the shared aim of increasing machining process efficiency [7].

## II. LITERATURE REVIEW

Authors Thiele and Melkote [7] investigated the influence of CBN insert edge geometry on the Ra of AISI 52100 hardened steel and determined that a larger re gives greater Ra than a smaller one. Similarly Chou and Song [8] were studied influence of re and concluded that lower re provided a bigger uncut thickness of chip, which increased temperature in the shear plane and formed deeper white layers, and vice versa. Siraj et al. [9] studied the effects of tribological parameters, re and found that the created empirical correlation could predict with an accuracy of 97.71% [0.4 mm re], 99.92% [0.8 mm re], and 99.67% [1.2 mm re].

Numerous authors studied the effect to dry and wet turning on hard materials. For [10] studied the coated carbide [B4C] under sliding and the results indicated that B4C coating considerably

reduce the sliding distance by 2m. Similarly [11] evaluated turning operations with hard materials in both dry and wet conditions utilizing HTMF. The study concluded that a large amount of the cutting fluid evaporated during chip production when a high velocity thin pulsed jet with an injection rate of only 3 ml/min was used. According to [12] evaluated SAE 52100 hardened steel with a minimal oil flow [10 ml/h] at various cutting speeds utilizing CBN inserts. After comparing dry and wet turning results, the study determined that flank wear was slightly lower in wet and Ra was comparable in both. The lowest Ra was reached at a cutting speed of 175 m/min, while lower cutting speeds had no effect on Ra or flank wear in both situations. According to [13] studied the effectiveness of several cooling strategies, including cryogenic cooling, MQL, NDM, HPC, and solid, liquid, and vapour coolants, in improving surface finish in turning with various inserts. The study found that cooling strategies extend the life of coated inserts such as ceramic, carbide, and CBN. Investigated the rheological and tribological properties of water-based lubricants in AISI 52100 bearing steels. The study showed that WBLs have increasing potential in the EV transportation sectors. It examined the role of high-pressure rheology and tribochemistry in wear mechanisms for several lubricants [14].

Many authors studied the effect of various inserts on surface roughness [Ra], tool wear [VB], material removal rate, etc. in hard turning operations. According to [15] used regression and neural networks as a predictive modeling approach to quantify Ra and VB using CBN insert. The study concluded that lowering the feed rate increases VB, but increasing roughness comes at the expense of increased VB. Additionally, honed edge geometry in CBN inserts delivers better outcomes in terms of Ra and VB during severe turning operations. Similarly For [16] investigated the effects of turning on hardened steel for automotive applications. The study examined the effects of several types of inserts, such as ceramics, carbide, CBN, and PCBN, on Ra, T, and VB. Tamizharasan et al. [17] investigated the Ra and VB of three types of CBN inserts on hardened materials used in crank pin manufacture. The study found that A-grade inserts had better Ra and T than low-grade CBN inserts. Used the Taguchi technique to optimize Ra and machining parameters in hard turning of AISI 1030 steel with titanium-nitrate coated insert. The study found that 1.2 mm re, 0.15 mm/rev f, and 0.5 mm d resulted in a 335% reduction in Ra when compared to the open literature [18]. According to [19] investigated the effect of machining parameters on hard turning of AISI 4140 steel at 51 HRC using a coated-carbide tool. The study found that feed rate had a substantial effect on Ra and Rz, as did the dual factor interaction. Hamdan et al. [20] improved the surface roughness of AISI 304 steel with a KORLOY coated carbide insert [APXT 11T3PDSR-MM]. The study was conducted with four input parameters utilizing a L9 orthogonal array, and the results showed a 25.3% reduction in cutting forces and a 41.3% rise in Ra. For [21] used a regression model to evaluate the tribological parameters of AISI 52100 steel [55 HRC] with carbide inserts. The study found that sharpened saw tooth chips in burnt blue have a substantial effect on Ra. The quadratic equation identified the optimal machining settings of ν, f and d as 70m/min, 0.04 mm/rev, and 0.1 mm respectively for achieving lower VB of 0.218 mm and 1.28 µm According to [22] investigated the dry turning operation on EN 31 steel with a CBN insert, optimizing the Ra and cutting tool settings. The study discovered that Ra increases with feed rate for all ν and d's under consideration. The optimal machining settings were determined to be ν, f, and d 100 m/min, 0.04 mm/rev, and 0.2 mm respectively.

Numerous authors were applied statistical and optimization techniques to optimize the machining parameters such as ν, f, d, re, cutting forces, and temperatures, etc. in hard turning operations. The investigated and compared the mistakes encountered in hard turning and grinding operations on hard materials [23]. The study discovered that hard turning delivers economic benefits on the basis of poorer precision as compared to grinding and superfinishing procedures. Similarly, for [24] investigated the 2D and 3D surface textures produced by rigorous turning and grinding processes. The study found that periodic-random surfaces based on 2D roughness were extremely unsafe. According to [25] used ANN to optimize Ra and tool wear in D2 hardened steel at 60 HRC. The study found that the multilayer precipitation model of ANN predicts with an accuracy of 0.979 and outperformed the multiple regression model. Chandrasekaran et al. [26] demonstrated using several computing approaches, such as ANN, GA, SA, and PSO, on four machining operations, including turning. The study found that PSO produced the best outcomes, followed by GA and ANN. According to [27] used a CBN implant to investigate AISI H11 steel with hardness varying from 40 to 50 HRC. The study used a four-factorial RSM approach for assessing Ra and the forces of cutting. The investigation found that feed and cutting forces significantly impacted the depth of cut [56.77% and 31.50%, respectively], but individual cutting speeds had only minor variances. For [28] used a multivariate statistical technique called principal component analysis to investigate surface finish in hard turning of AISI 52100 steel. The study concluded that using the Ra and Rt components of PCA to make decisions about the optimal parameters of hard turning, while reducing VB reduces Ra. According to [29] investigated the effect of machining settings on dry hard turning with CBN inserts using the MCDM approach TOPSIS. ANOVA analysis revealed that the optimal parameters for achieving 0.507 µm Ra were ν, f, and d at 200/min, 0.1 mm/rev, 0.8 mm, and 1.2 mm re. According to [30] studied the impact of machining settings on AISI 52100 steel using the Box-Behnken design. The study found that temperature and power consumption had a substantial impact on the machining parameters measured in the FEM analysis. At the minimal conditions, the ν, f, and d were 162.42 m/min, 0.247 mm/rev, and 1.395 mm, respectively.

Few authors also studied the various techniques to enhance the Ra in hard turning operations. For [31] investigated the Ra in PHT of AISI 52100 steel [60-62 HRC] with a CBN insert in relation to rolling contact fatigue. The study found a very fine white coating [<1µm] on the top surface and increased residual stresses in PHT, with a negligible effect on microstructural phases. RCF life rises at the expense of Ra degradation. Similarly, [32] proposed a new technique for determining VB using sonic emission signals in AISI 4340 steel. The investigation was carried out on coated and uncoated nanostructured AlCrN carbide inserts, and the study found that increasing the amplitude of power resulted in an increase in VB and density at the end of VB. According to [33] investigated the Ra optimization technique for AISI 1053 steel utilizing the Johnson-Cook constant and wear factors. The study found that the 3D oblique cutting forces model had a stronger relationship with the flank wear model, but Ra predicted using the empirical model differed significantly from the experimental results. For [34] investigated the UVAT machining technique using a coated-carbide insert in hard turning of 62 HRC steel. The study found that using these techniques resulted in a lower Ra of 1.12µm than standard turning operations. Studied machining parameters to study VB in AISI 52100 steel utilizing a long-term approach of solid-lubricant assisted machining [SLAM] in dry turning. The study found that the SLAM technique dramatically reduced cutting

forces, vibrations, VB, and Ra by 60%, 29%, 17%, and 66%, respectively [35].

The current study attempts to investigate the influence of coated carbide inserts on hardened material with a hardness of 47 HRC. The experiment was designed utilizing the Box-Behnken approach of the RSM method to optimize surface roughness under varied machining parameters, including re circumstances. A total of 27 runs were calculated using the considered method, and graphs for estimated and experimental surface roughness are presented.

## III. MATERIALS AND METHODS

The experimental program begins with material selection for experimentation, followed by machining parameters selection, turning processes (dry and wet), surface roughness, and optimization approach. Machinability in hard turning processes is affected by a number of elements, including the machine, tool, cutting, and workpiece. The current study focuses primarily on tool material and geometry, ν, f, and d, re, and material hardness. The experimentation has been performed on EN31 material formally known as bearing steel. The chemical composition and ranges for EN31 steel are given in Table 1. While executing machining operations, three different levels are chosen ranging from -1 to +1 for the machining parameters being considered. The machining parameters and levels are listed in Table 2.

Table 1: Chemical composition and ranges for EN31

| Chemical Composition | Range (%) |
|---|---|
| Carbon | 0.98-1.10 |
| Manganese | 0.25-0.45 |
| Chromium | 1.30-1.60 |
| Silicon | 0.15-0.30 |
| Sulphur | 0.025 max. |
| Phosphorous | 0.025 max. |
| Nickel | - |
| Molybdenum | - |

Source: Authors, (2024).

Table 2: Machining parameters and their levels

| Parameters | Units | Levels | | |
|---|---|---|---|---|
| | | -1 | 0 | +1 |
| Cutting Speed (ν) | m/min | 160 | 210 | 260 |
| Feed (f) | mm/rev | 0.1 | 0.15 | 0.2 |
| Depth of cut (d) | mm | 0.05 | 0.1 | 0.15 |
| Tool Nose Radius ($r_e$) | mm | 0.4 | 0.8 | 1.2 |

Source: Authors, (2024).

The raw EN 31 material's hardness was assessed using a Rockwell hardness tester and was determined to be between 25 and 27 HRC. Further raw materials were split into 27 samples for the hardening operation. At the preparatory stage, all 27 EN31 samples were faced and plane turned, followed by a hardening process. Again, the hardness of all the samples was assessed and found to be between 46 and 47 HRC, and runs were calculated using the Box-Behnken approach of the response surface method, which included ν, f, d, and re. The experiment is carried out using a 25 mm diameter EN31 material measuring 60 mm in length. To improve the accuracy of the turning operation, a center hole is drilled in each sample. The Ra of each sample is tested three times using a Mitutoyo surface roughness tester, and the average value has been utilized for computations. The number of runs in the current study is computed using RSM's Box-Behnken technique. A total 27 runs are calculated using the machining parameters under consideration, and a quadratic equation is produced for surface roughness. Table 3 shows the run table for the Box-Behnken technique, which includes the estimated and actual values of machining parameters as well as standard and run orders. The table also shows the experimental and estimated Ra using quadratic equations, along with their percentage errors for each sample.
Quadratic Equation:

$$R_a = -0.674 + 0.015v + 6.193f + 5.436d - 1.061r_e - 0.016v \times f - 0.012v \times d + 0.0005v \times r_e + 1.00f \times d + 8.508 \times 10^{-15} f \times r_e + 0.125d \times r_e - 0.000012v^2 - 2.166f^2 - 1.666d^2 + 0.044r_e^2 \quad (1)$$

Table 3: Run table for hard turning using Box-Behnken approach of RSM.

| Std Order | Run Order | ν | f | d | $r_e$ | Ra (Exp) | Ra (Est) | % Error |
|---|---|---|---|---|---|---|---|---|
| 22 | 1 | 210 | 0.2 | 0.1 | 0.4 | 2.57 | 2.55 | 0.78 |
| 12 | 2 | 260 | 0.15 | 0.1 | 1.2 | 2.15 | 2.12 | 1.40 |
| 3 | 3 | 160 | 0.2 | 0.1 | 0.8 | 1.80 | 1.82 | 1.11 |
| 15 | 4 | 210 | 0.1 | 0.15 | 0.8 | 2.11 | 2.11 | 0.00 |
| 18 | 5 | 260 | 0.15 | 0.05 | 0.8 | 2.35 | 2.34 | 0.43 |
| 1 | 6 | 160 | 0.1 | 0.1 | 0.8 | 1.54 | 1.51 | 1.95 |
| 19 | 7 | 160 | 0.15 | 0.15 | 0.8 | 1.82 | 1.84 | 1.10 |
| 14 | 8 | 210 | 0.2 | 0.05 | 0.8 | 2.06 | 2.05 | 0.49 |
| 10 | 9 | 260 | 0.15 | 0.1 | 0.4 | 2.81 | 2.80 | 0.36 |
| 23 | 10 | 210 | 0.1 | 0.1 | 1.2 | 1.61 | 1.63 | 1.24 |
| 21 | 11 | 210 | 0.1 | 0.1 | 0.4 | 2.32 | 2.33 | 0.43 |
| 17 | 12 | 160 | 0.15 | 0.05 | 0.8 | 1.52 | 1.49 | 1.97 |
| 24 | 13 | 210 | 0.2 | 0.1 | 1.2 | 1.86 | 1.86 | 0.00 |
| 26 | 14 | 210 | 0.15 | 0.1 | 0.8 | 2.09 | 2.09 | 0.00 |
| 9 | 15 | 160 | 0.15 | 0.1 | 0.4 | 2.02 | 2.04 | 0.99 |
| 13 | 16 | 210 | 0.1 | 0.05 | 0.8 | 1.81 | 1.83 | 1.10 |
| 6 | 17 | 210 | 0.15 | 0.15 | 0.4 | 2.59 | 2.58 | 0.39 |
| 27 | 18 | 210 | 0.15 | 0.1 | 0.8 | 2.09 | 2.09 | 0.00 |
| 7 | 19 | 210 | 0.15 | 0.05 | 1.2 | 1.58 | 1.60 | 1.27 |
| 20 | 20 | 260 | 0.15 | 0.15 | 0.8 | 2.53 | 2.56 | 1.19 |
| 2 | 21 | 260 | 0.1 | 0.1 | 0.8 | 2.38 | 2.37 | 0.42 |
| 4 | 22 | 260 | 0.2 | 0.1 | 0.8 | 2.48 | 2.52 | 1.61 |
| 25 | 23 | 210 | 0.15 | 0.1 | 0.8 | 2.09 | 2.09 | 0.00 |
| 5 | 24 | 210 | 0.15 | 0.05 | 0.4 | 2.29 | 2.30 | 0.44 |
| 11 | 25 | 160 | 0.15 | 0.1 | 1.2 | 1.32 | 1.32 | 0.00 |
| 16 | 26 | 210 | 0.2 | 0.15 | 0.8 | 2.37 | 2.34 | 1.27 |
| 8 | 27 | 210 | 0.15 | 0.15 | 1.2 | 1.89 | 1.89 | 0.00 |

Source: Authors, (2024).

## IV. RESULTS AND DISCUSSIONS

The results focuses primarily on experimental data, such as machining parameters versus Ra. Additional findings based on Box-Behnken design are presented about the effect of combined machining parameters on Ra. Finally, it includes a comparison of experimental and estimated Ra using standard error. During wet turning, Ra is estimated using a variety of machining parameters, including ν, f, d, and re. Figure 1 shows a box plot for various machining parameters and Ra. Figure 1(a) depicts the relationship between ν and Ra, while 1(b), 1(c), and 1(d) show the relationship between f, dc, and re against Ra, respectively.

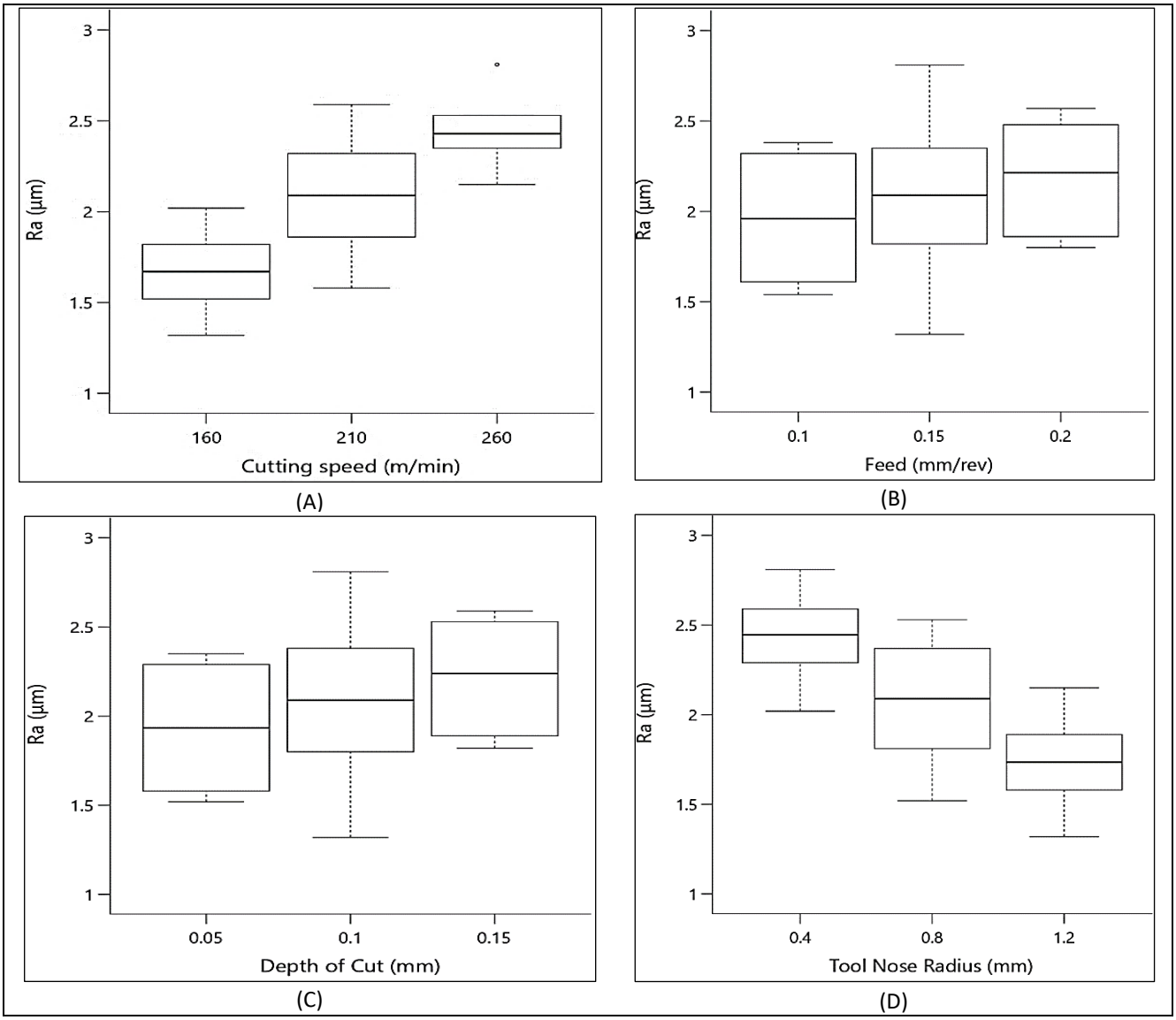


Figure 1: Comparison of Machining Parameters versus Surface Roughness:
a – Cutting speed vs Ra; b – Feed vs Ra;
c – Depth of cut vs Ra; d – Tool Nose Radius vs Ra.
Source: Authors, (2024).

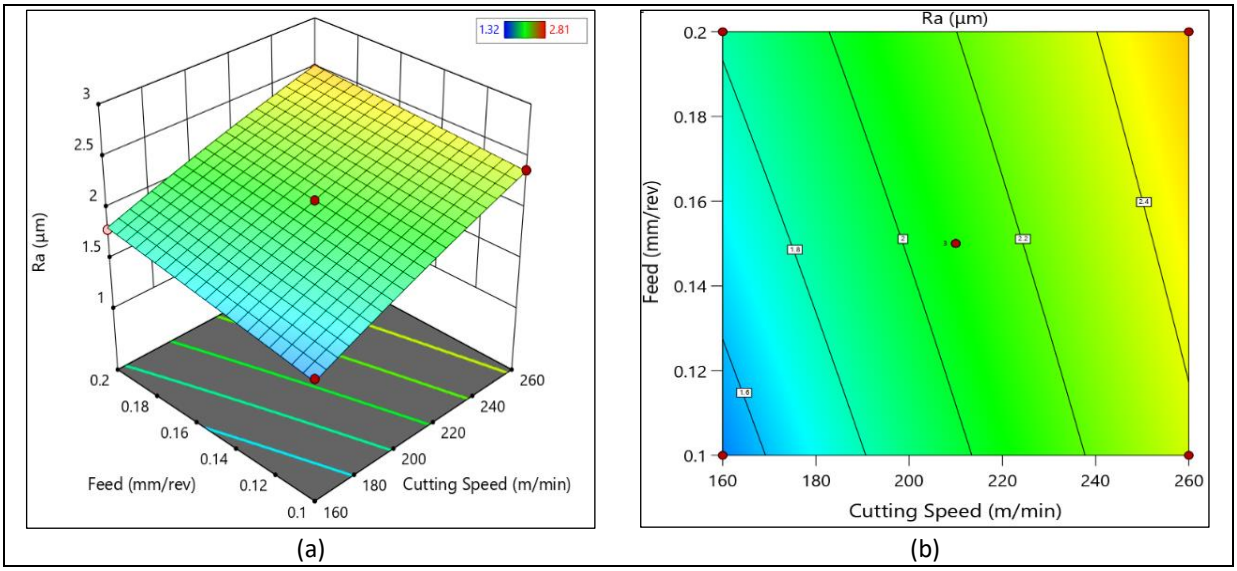


Figure: 2 Response diagram of v and f versus Ra.
a – Feed and Cutting speed vs Ra; b – Contour plot.
Source: Authors, (2024).

Figure 1(a) shows that ν increases as Ra increases. At lower ν (160 m/min) Ra observed within the range of 1.5-1.8 µm whereas for 210 and 260 m/min observed within the range of 1.9-2.4 µm and 2.4-2.5 µm. At higher ν, the interquartile range is very closer and an outlier is observed for Ra near 3 µm. Similarly 1(b) and 1(c) shows that marginal variations in Ra for the range of f and d under consideration. Ra is observed within the range of 1.5-2.5 µm for both machining parameters and significant variations are observed for whiskers at 0.15 mm/rev f and 0.1 mm d in comparison with others. Figure 1(d) illustrates the relation between re and Ra. Ra decreases as re increases. The Ra is observed within the range of 1.4 to 2.9 µm and the interquartile range is observed larger at 0.8 mm re. The chip forming mechanism has a vital influence in Ra and re. A larger re lowers chip formation while improving Ra. Many researches have confirmed the relationship between Ra and re.

The number of runs in an experiment is computed using the Box-Behnken design of response surface approaches. The experimental application generates 3D response graphs and contour plots for machining parameters versus Ra. Figure 2 depicts the response diagram of f and ν versus Ra. A 3D surface plot is observed in Figure 2(a) while Figure 2(b) shows contour plot. A decreasing trend is observed in Ra when compared with f and ν. Figure 2(a) clearly shows that lower Ra is at 0.1 mm/rev f and 160 m/min ν, while Ra increases with increase in f and ν. The highest 2.8 µm Ra is observed when both machining parameters are set to higher levels. Contour plot 2(b) shows an increasing trend of Ra from 1.6 to 2.4 µm in relation to ν and f for all runs considered. A considerable contribution of f and ν is observed in turning operations. From the investigated range of both machining parameters, the least values give enhanced Ra leading to minimizing the intensity of forces and generation of heat at the surface.

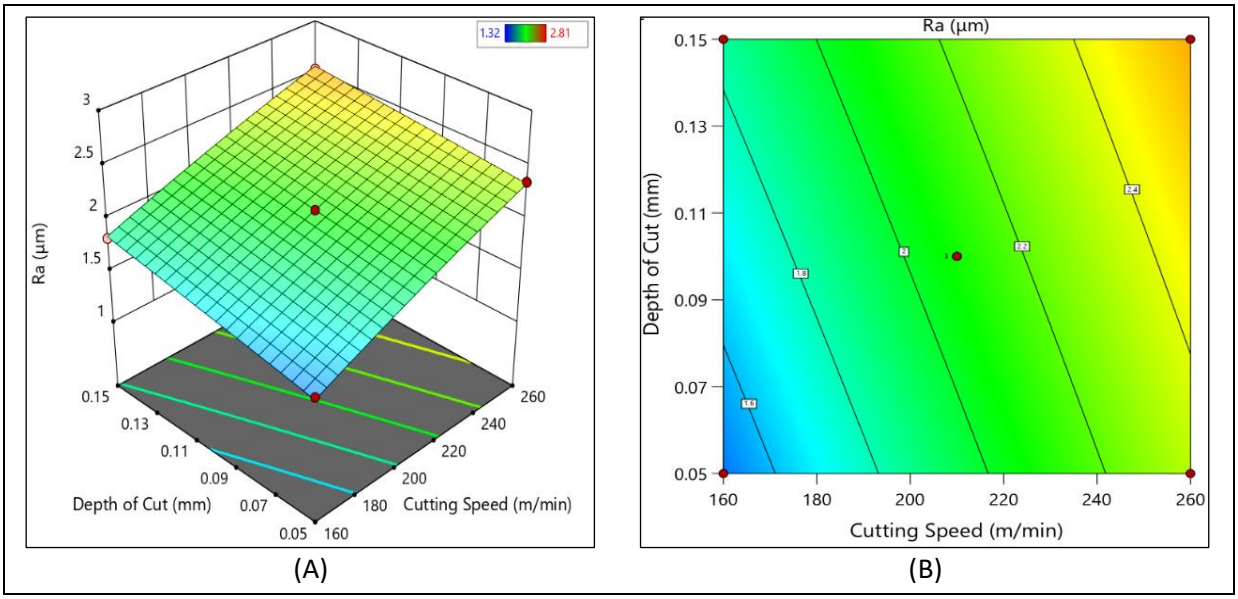


Figure 3: Response diagram of ν and d versus Ra.
a – Depth of cut and Cutting speed vs Ra; b – Contour plot.
Source: Authors, (2024).

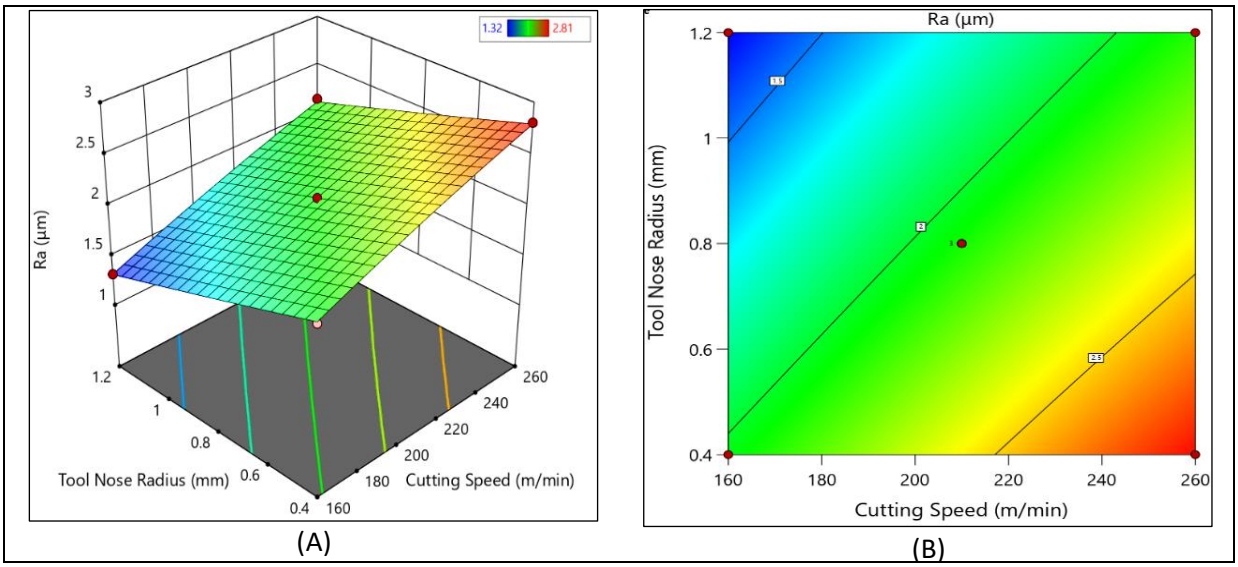


Figure 4: Response diagram of ν and re versus Ra.
a – Tool nose radius and Cutting speed vs Ra; b – Contour plot.
Source: Authors, (2024).

Figure 3 depicts the response diagram of ν and d versus Ra. A similar trend like Figure 2 is observed in this section. Figure 3(a) shows the lowest Ra at 0.05 mm d and 160 m/min ν. If both the machining parameters are set to its higher levels provide greater Ra value 2.8 µm. Figure 3(b) also shows similar trend like Figure 2(b), an increasing trend of Ra from 1.6 to 2.4 µm in relation to ν and f for all runs considered. In turning operations, both d and ν play an important role. A smaller d improves Ra by removing less material per pass, resulting in less vibrations and resistance in tool materials.

Figure 4 depicts the response diagram of re and ν versus Ra. A 3D surface plot is observed in Figure 4(a) while Figure 4(b) shows contour plot. A decreasing trend in Ra with increase in re is observed and increasing in Ra with increase in ν is observed in Figure 4(a). Similar to a reduced d, a lower re with a lower ν significantly reduces Ra by removing fewer materials, but an increase in re with a lower ν increases Ra. At faster ν's and a smaller re, the tool material experiences more forces, vibrations, and resistance. From contour plot 4(b), the lowest Ra's are observed above 1 mm re whereas highest observed at above 220 m/min ν.

Figure 5 depicts the response diagram of d and f versus Ra. A 3D surface plot is observed in Figure 5(a) while Figure 5(b) shows contour plot. The deviations in f and d provides marginal variations Ra for all the runs under considerations. Some of the researches showed that the f significantly affects the Ra leading to increase in forces and vibrations in tool materials, but d do not have significant impact on forces and Ra. The Ra is observed within the range of 1.9 to 2.3 µm for both increase in f and d.

Figure 6 depicts the response diagram of re and f versus Ra. A 3D surface plot is observed in Figure 6(a) while Figure 6(b) shows contour plot. A decreasing trend in Ra with increase in re is observed and increasing in Ra with decrease in f is observed in Figure 6(a). The Ra is observed within the range of 1.8 to 2.4 µm for all the runs under considerations. From contour plot 6(b), the lowest Ra are observed above 1 mm re whereas highest observed at above 0.14 mm/rev f.

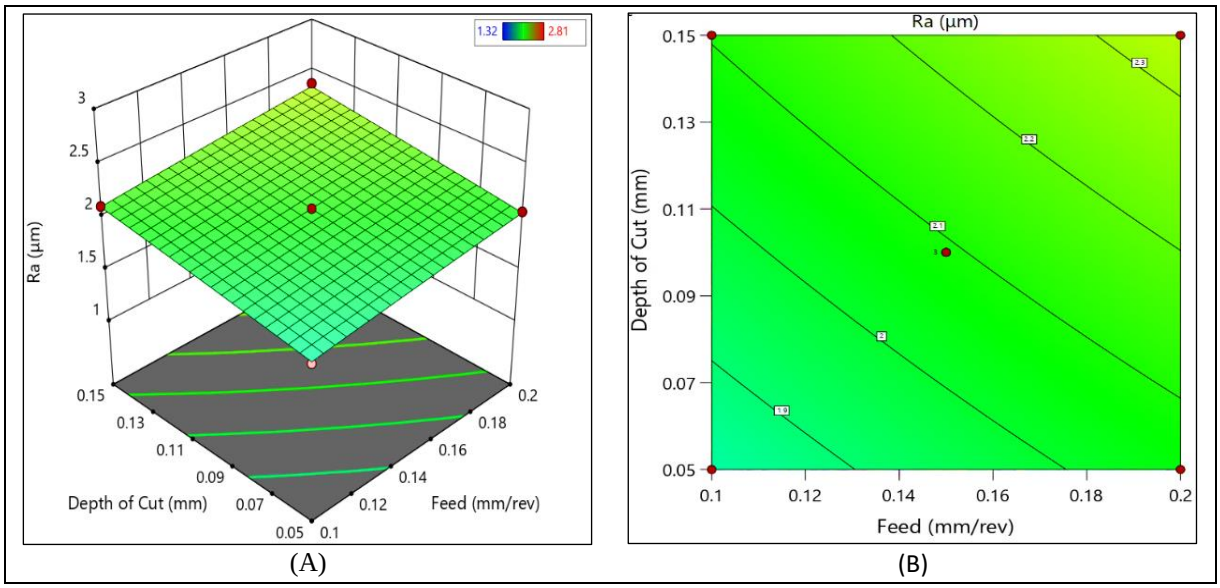


Figure 5: Response diagram of f and d versus Ra.
a – Depth of cut and Feed vs Ra; b – Contour plot.
Source: Authors, (2024).

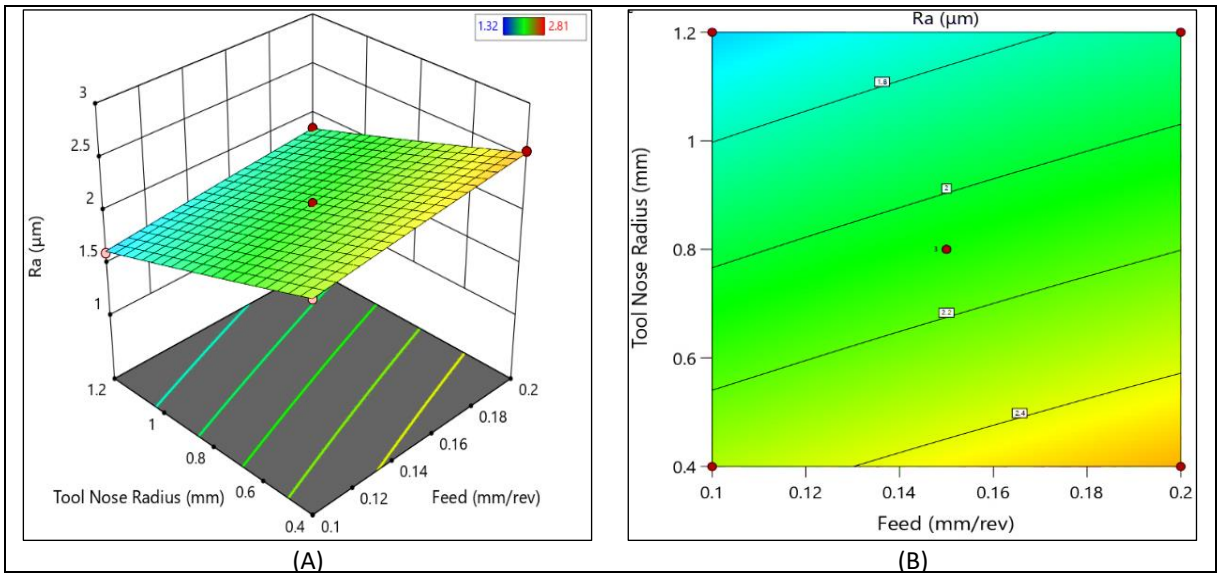


Figure 6: Response diagram of f and re versus Ra.
a – Tool nose radius and Feed vs Ra; b – Contour plot.
Source: Authors, (2024).

Figure 7 depicts the response diagram of re and d versus Ra. A 3D surface plot is observed in Figure 7(a) while Figure 7(b) shows contour plot. Similar to the Figure 6, a decreasing trend in Ra with increase in re is observed and increasing in Ra with decrease in d is observed in Figure 6(a). The Ra is observed within the range of 1.8 to 2.4 µm for all the runs under considerations. From contour plot 7(b), the lowest Ra's are observed above 1 mm re whereas highest observed at above 0.09 mm d.

Figure 8 shows a comparison of experimental and estimated Ra for all runs under investigation. The experimental value of Ra was measured three times and the average was used in computations. The expected Ra is anticipated using the quadratic equation obtained from the Box-Behnken method of the RSM approach. A substantial interconnectivity is observed between experimental and calculated Ra, and values predicted using a quadratic equation exhibit accuracy of prediction $R^2$=0.9976. Anova for the quadratic model yields a face value of 356.21, indicating that the developed model is noteworthy. Individual machining parameters such as ν, f, d, and re, as well as combinations of parameters such as ν and f, ν and d, and ν into ν, have a substantial effect on Ra. The remaining quadratic equation parameters had a minor effect on Ra and were observed using P-values.

Figure 9 displays f and ν versus design errors. Figure 9(a) shows a 3D surface plot, while 9(b) provides a contour plot of the same. Figure 9(a) and 9(b) clearly show that the outer margins of the surface plot have large inaccuracies, but the intensity reduces as one moves closer to the centroidal point. An asymptotic tendency is seen between 180 and 240 m/min ν and 0.12-0.18 mm/rev f. The similar results are also observed in different combinations of machining parameters. The percentage errors are in the range of 1.613-1.974%.

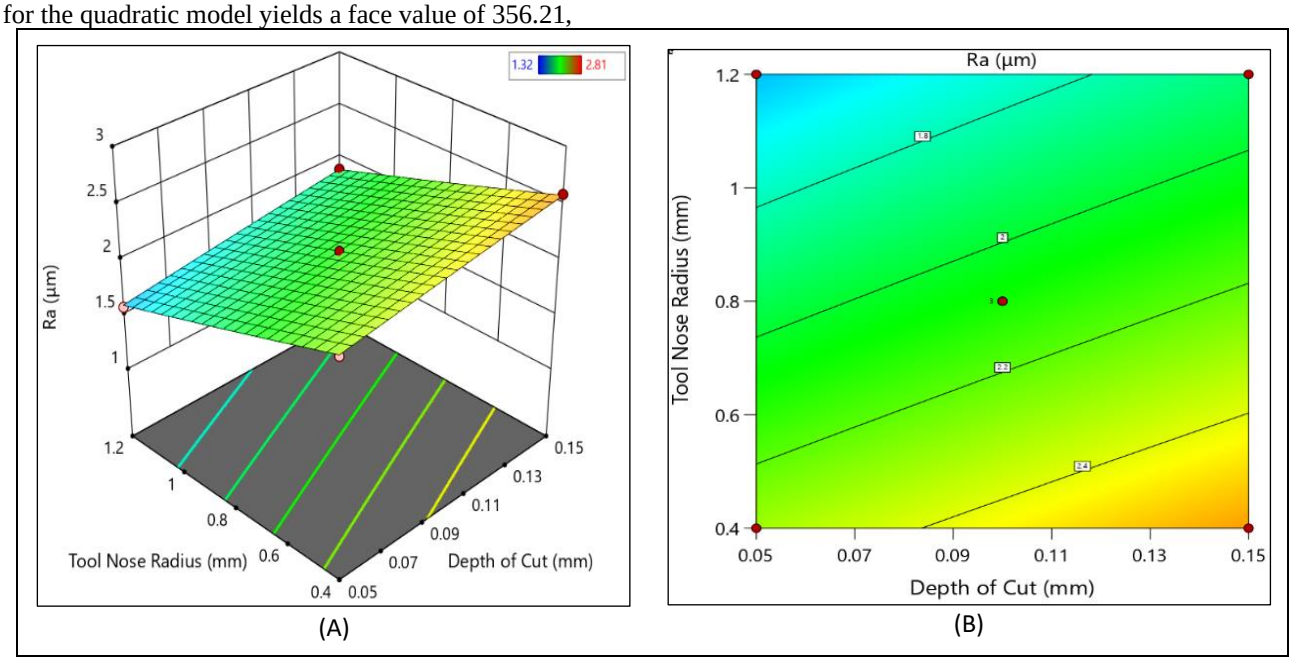


Figure 7: Response diagram of d and re versus Ra.
a – Tool nose radius and Depth of cut vs Ra; b – Contour plot.
Source: Authors, (2024).

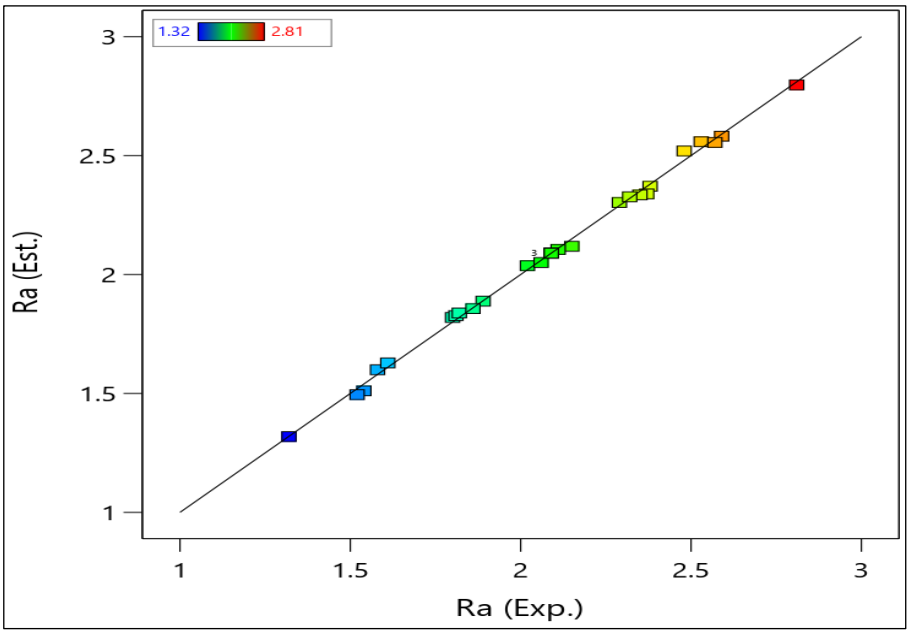


Figure 8: Comparison of Ra (Exp.) versus Ra (Est.).
Source: Authors, (2024).

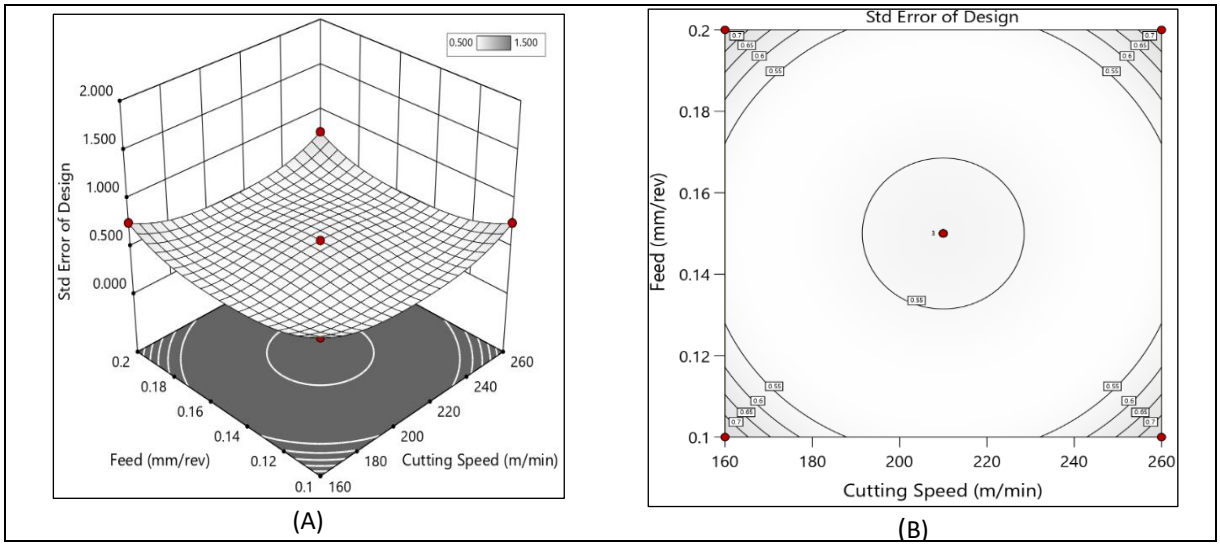


Figure 9: Response diagram of v and f versus Standard error of design:
a – Feed and Cutting speed vs Std. error of design; b – Contour plot.
Source: Authors, (2024).

The discussion based on current research work mainly focused on the problem statements and the conclusive findings from the current research. From the experimentation it has been observed that surface finish increases with increase in cutting speed, feed rate, and depth of cut, whereas it decreases with increase in tool nose radius. Several factors such as thermal expansion, built-up edge, chatter marks, contact timings and vibration may lead to increase the surface roughness due to increased cutting speed. The primary goal of the current research work was to use coated carbide inserts to optimize the surface finish of hardened EN31 alloy steel. The RSM Box-Behnken technique was used to formulate the procedure. The Box-Behnken approach yielded results in the form of contour plots, and it was noted how the machining parameters impacted the surface finish. Lower feed rate, depth of cut and cutting speed provides the excellent surface finish, this may be attributed due to fewer pass timings, heat generations and balanced forces. Larger contact area, which promotes smoother operation and balanced forces, may be the reason why higher tool nose radius combined with lower cutting rates improves surface smoothness. A sharper edge produced by a lower tool nose radius increases the intensity of cutting forces. The tight range of both feed rate and depth of cut may be the reason for the minor effects they have on surface roughness. Similar trends may be seen in the prediction of surface finish between tool nose radius and feed rate, as well as tool nose radius and depth of cut. Surface finish is not significantly affected by feed rate or depth of cut; instead, it is reduced by lower feed rate and depth of cut combined with a larger tool nose radius. The cutting forces' balancing may be the cause of this.

## V. CONCLUSIONS

The experimentation on EN31 material was carried out with a coated carbide insert, and runs were estimated using the Box-Behnken approach of RSM. The machining parameters v, f, d, and re are all considered inputs, whereas Ra is predicted using the input parameters as a function. The conclusions are based on testing and optimization utilizing the Box-Behnken technique:

- The machining parameters v, f, d, and re significantly affects the Ra and it is observed within the range of 1.34-2.81 µm for all the runs under considerations.
- The Ra shows a decreasing tendency as compared to re, but an increasing trend with the remaining machining parameters.
- Reduced force intensity, heat generation, and fewer material per pass, forces and vibrations are noted at reduced v and f, and d with a larger re, resulting in smaller Ra.
- Marginal variations are observed in Ra when compared with d and f.
- The individual and combined effect of machining parameters on Ra are identified by considering p-value <0.05.
- The quadratic equation predicts Ra with an accuracy of R2=0.9976 and Anova model offers face value of 356.21 indicates the developed model is noteworthy.
- The errors are observed within the range of 1.613-1.974%. The Box-Behnken approach of RSM played a key role in optimizing machining parameters in hard turning.

## VI. AUTHOR'S CONTRIBUTION

**Conceptualization:** Shivaji Bhivsane, Arvind Chel and Siraj Sayyed.
**Methodology:** Shivaji Bhivsane, Arvind Chel and Siraj Sayyed.
**Investigation:** Shivaji Bhivsane, Arvind Chel and Siraj Sayyed.
**Discussion of results:** Shivaji Bhivsane, Arvind Chel and Siraj Sayyed.
**Writing – Original Draft:** Shivaji Bhivsane, Arvind Chel and Siraj Sayyed.
**Writing – Review and Editing:** Shivaji Bhivsane, Arvind Chel and Siraj Sayyed.
**Resources:** Shivaji Bhivsane, Arvind Chel and Siraj Sayyed.
**Supervision:** Shivaji Bhivsane, Arvind Chel and Siraj Sayyed.
**Approval of the final text:** Shivaji Bhivsane, Arvind Chel and Siraj Sayyed.

## VII. ACKNOWLEDGMENTS

Authors are thankful to the management of MIT College, Aurangabad for providing research facility.

## VIII. REFERENCES

[1] D. Anoop, A. S. Sekhar, M. Kamaraj, and K. Gopinath, "Numerical evaluation of subsurface stress field under elastohydrodynamic line contact for AISI 52100 bearing steel with retained austenite," Wear, vol. 330–331, pp. 636–642, 2015, doi: 10.1016/j.wear.2015.01.021.

[2] Attanasio, D. Umbrello, C. Cappellini, G. Rotella, and R. M'Saoubi, "Tool wear effects on white and dark layer formation in hard turning of AISI 52100 steel," Wear, vol. 286–287, pp. 98–107, 2012, doi: 10.1016/j.wear.2011.07.001.

[3] D. Bagawade, P. G. Ramdasi, R. S. Pawade, and P. K. Bramhankar, "Evaluation of Cutting Forces in Hard Turning of Aisi 52100 Steel By Using Taguchi Method," vol. 1, no. 6, pp. 1–5, 2012.

[4] G. Bartarya and S. K. Choudhury, "Effect of Cutting Parameters on Cutting Force and Surface Roughness During Finish Hard Turning AISI52100 Grade Steel," Procedia CIRP, vol. 1, no. mm, pp. 651–656, 2012, doi: 10.1016/j.procir.2012.05.016.

[5] I. S. Cho, A. Amanov, and J. D. Kim, "The effects of AlCrN coating, surface modification and their combination on the tribological properties of high speed steel under dry conditions," Tribol. Int., vol. 81, pp. 61–72, 2015, doi: 10.1016/j.triboint.2014.08.003.

[6]Y. B. Guo and C. R. Liu, "Mechanical properties of hardened AISI 52100 steel in hard machining processes," J. Manuf. Sci. Eng., vol. 124, no. 1, pp. 1–9, 2002, doi: 10.1115/1.1413775.

[7] J. D. Thiele and S. N. Melkote, "Effect of cutting edge geometry and workpiece hardness on surface generation in the finish hard turning of AISI 52100 steel," J. Mater. Process. Technol., vol. 94, no. 2, pp. 216–226, 1999, doi: 10.1016/S0924-0136(99)00111-9.

[8] Y. K. Chou and H. Song, "Tool nose radius effects on finish hard turning," J. Mater. Process. Technol., vol. 148, no. 2, pp. 259–268, 2004, doi: 10.1016/j.jmatprotec.2003.10.029.

[9] S. Siraj, H. M. Dharmadhikari, and N. Gore, "Modeling of Roughness Value from Tribological Parameters in Hard Turning of AISI 52100 Steel," Procedia Manuf., vol. 20, pp. 344–349, 2018, doi: 10.1016/j.promfg.2018.02.050.

[10] S. J. Harris, G. Krauss, M. T. Siniawski, Q. Wang, S. Liu, and Y. Ao, "Surface feature variations observed in 52100 steel sliding against a thin boron carbide coating," Wear, vol. 249, no. 10–11, pp. 1004–1013, 2001, doi: 10.1016/S0043-1648(01)00840-7.

[11] A. S. Varadarajan, P. K. Philip, and B. Ramamoorthy, "Investigations on hard turning with minimal cutting fluid application (HTMF) and its comparison with dry and wet turning," Int. J. Mach. Tools Manuf., vol. 42, no. 2, pp. 193–200, 2002, doi: 10.1016/S0890-6955(01)00119-5.

[12] E. Diniz, J. R. Ferreira, and F. T. Filho, "Influence of refrigeration/lubrication condition on SAE 52100 hardened steel turning at several cutting speeds," Int. J. Mach. Tools Manuf., vol. 43, no. 3, pp. 317–326, 2003, doi: 10.1016/S0890-6955(02)00186-4.

[13] V. S. Sharma, M. Dogra, and N. M. Suri, "Cooling techniques for improved productivity in turning," Int. J. Mach. Tools Manuf., vol. 49, no. 6, pp. 435–453, 2009, doi: 10.1016/j.ijmachtools.2008.12.010.

[14 J. Bosch and C. DellaCorte, "Rheological Characterization and Tribological Evaluation of Water-Based Lubricants in AISI 52100 Bearing Steel," Tribol. Lett., vol. 72, no. 1, 2024, doi: 10.1007/s11249-023-01811-7.

[15] T. Özel and Y. Karpat, "Predictive modeling of surface roughness and tool wear in hard turning using regression and neural networks," Int. J. Mach. Tools Manuf., vol. 45, no. 4–5, pp. 467–479, 2005, doi: 10.1016/j.ijmachtools.2004.09.007.

[16] S. K. Shihab, Z. A. Khan, A. Mohammad, and A. N. Siddiquee, "A review of turning of hard steels used in bearing and automotive applications," Prod. Manuf. Res., vol. 2, no. 1, pp. 24–49, 2014, doi: 10.1080/21693277.2014.881728.

[17] T. Tamizharasan, T. Selvaraj, and A. N. Haq, "Analysis of tool wear and surface finish in hard turning," Int. J. Adv. Manuf. Technol., vol. 28, no. 7–8, pp. 671–679, 2006, doi: 10.1007/s00170-004-2411-1.

[18] M. Nalbant, H. Gökkaya, and G. Sur, "Application of Taguchi method in the optimization of cutting parameters for surface roughness in turning," Mater. Des., vol. 28, no. 4, pp. 1379–1385, 2007, doi: 10.1016/j.matdes.2006.01.008.

[19] I. Asiltürk and H. Akkuş, "Determining the effect of cutting parameters on surface roughness in hard turning using the Taguchi method," Meas. J. Int. Meas. Confed., vol. 44, no. 9, pp. 1697–1704, 2011, doi: 10.1016/j.measurement.2011.07.003.

[20] A. Hamdan, A. A. D. Sarhan, and M. Hamdi, "An optimization method of the machining parameters in high-speed machining of stainless steel using coated carbide tool for best surface finish," Int. J. Adv. Manuf. Technol., vol. 58, no. 1–4, pp. 81–91, 2012, doi: 10.1007/s00170-011-3392-5.

[21] Panda, A. K. Sahoo, and A. K. Rout, "Statistical regression modeling and machinability study of hardened AISI 52100 steel using cemented carbide insert," Int. J. Ind. Eng. Comput., vol. 8, no. 1, pp. 33–44, 2017, doi: 10.5267/j.ijiec.2016.7.004.

[22] M. S. Karthik, V. R. Raju, K. Niranjan Reddy, N. Balashanmugam, and M. R. Sankar, "Cutting parameters optimization for surface roughness during dry hard turning of EN 31 bearing steel using CBN insert," Mater. Today Proc., vol. 26, no. xxxx, pp. 1119–1125, 2019, doi: 10.1016/j.matpr.2020.02.224.

[23] J. Kundrák, B. Karpuschewski, K. Gyani, and V. Bana, "Accuracy of hard turning," J. Mater. Process. Technol., vol. 202, no. 1–3, pp. 328–338, 2008, doi: 10.1016/j.jmatprotec.2007.09.056.

[24] W. Grzesik, K. Żak, and P. Kiszka, "Comparison of surface textures generated in hard turning and grinding operations," Procedia CIRP, vol. 13, pp. 84–89, 2014, doi: 10.1016/j.procir.2014.04.015.

[25] R. Quiza, L. Figueira, and J. P. Davim, "Comparing statistical models and artificial neural networks on predicting the tool wear in hard machining D2 AISI steel," Int. J. Adv. Manuf. Technol., vol. 37, no. 7–8, pp. 641–648, 2008, doi: 10.1007/s00170-007-0999-7.

[26] M. Chandrasekaran, M. Muralidhar, C. M. Krishna, and U. S. Dixit, "Application of soft computing techniques in machining performance prediction and optimization: A literature review," Int. J. Adv. Manuf. Technol., vol. 46, no. 5–8, pp. 445–464, 2010, doi: 10.1007/s00170-009-2104-x.

[27] H. Aouici, M. A. Yallese, K. Chaoui, T. Mabrouki, and J. F. Rigal, "Analysis of surface roughness and cutting force components in hard turning with CBN tool: Prediction model and cutting conditions optimization," Meas. J. Int. Meas. Confed., vol. 45, no. 3, pp. 344–353, 2012, doi: 10.1016/j.measurement.2011.11.011.

[28] G. Evangelista, R. S. Peruchi, T. G. Brito, P. R. Junior, and L. C. S. Rocha, "A Multivariate Statistical Quality Control of AISI 52100 Hardened Steel Turning," IEEE Access, vol. 8, no. June, pp. 109092–109104, 2020, doi: 10.1109/ACCESS.2020.3000585.

[29] P. Umamaheswarrao, D. Rangaraju, K. N. S. Suman, and B. Ravisankar, "Application of TOPSIS for multi response optimization of Process Parameters in dry hard turning of AISI 52100 steel," INCAS Bull., vol. 13, no. 1, pp. 211–224, 2021, doi: 10.13111/2066-8201.2021.13.1.22.

[30] A. Yıldız, L. Uğur, and İ. E. Parlak, "Optimization of the Cutting Parameters Affecting the Turning of AISI 52100 Bearing Steel Using the Box-Behnken Experimental Design Method," Appl. Sci., vol. 13, no. 1, 2023, doi: 10.3390/app13010003.

[31] N. Jouini, P. Revel, G. Thoquenne, and F. Lefebvre, "Characterization of surfaces obtained by Precision Hard Turning of AISI 52100 in relation to RCF life," Procedia Eng., vol. 66, pp. 793–802, 2013, doi: 10.1016/j.proeng.2013.12.133.

[32] L. H. A. Maia, A. M. Abrao, W. L. Vasconcelos, W. F. Sales, and A. R. Machado, "A new approach for detection of wear mechanisms and determination of tool life in turning using acoustic emission," Tribol. Int., vol. 92, pp. 519–532, 2015, doi: 10.1016/j.triboint.2015.07.024.

[33] J. Zhang, S. Y. Liang, J. Zhang, and S. Y. Liang, "Process Optimization of Finish Turning of Hardened Steels," vol. 6914, no. January, 2016, doi: 10.1080/10426910601016020.

[34] G. S. Ghule, S. Sanap, S. Adsul, S. Chinchanikar, and M. Gadge, "Experimental investigations on the ultrasonic vibration-assisted hard turning of AISI 52100 steel using coated
carbide tool," Mater. Today Proc., vol. 68, pp. 2093–2098, 2022, doi: https://doi.org/10.1016/j.matpr.2022.08.368.

[35] Borgaonkar and I. Syed, "Tool wear analysis in AISI 52100 steel machining with sustainable approach," Mater. Manuf. Process., vol. 39, no. 10, pp. 1369–1379, 2024, doi: 10.1080/10426914.2024.2323437.